

Enhanced Proton Conduction in Polymer Electrolyte Membranes as Synthesized by Polymerization of Protic Ionic Liquid-Based Microemulsions

Feng Yan,^{*,†,‡} Shaomei Yu,[†] Xingwang Zhang,[§] Lihua Qiu,[†] Fuqiang Chu,[†] Jingbi You,[§] and Jianmei Lu^{*,†}

Key Laboratory of Organic Synthesis of Jiangsu Province, School of Chemistry and Chemical Engineering, Soochow University, Suzhou 215123, P. R. China, Key Laboratory of Molecular Engineering of Polymers, Fudan University, P. R. China, Key Laboratory of Semiconductor Materials Science, Institute of Semiconductors, Chinese Academy of Sciences, Beijing 100083, P. R. China

Received January 13, 2009. Revised Manuscript Received March 3, 2009

Proton-conducting membranes were prepared by polymerization of microemulsions consisting of surfactant-stabilized protic ionic liquid (PIL) nanodomains dispersed in a polymerizable oil, a mixture of styrene and acrylonitrile. The obtained PIL-based polymer composite membranes are transparent and flexible even though the resulting vinyl polymers are immiscible with PIL cores. This type of composite membranes have quite a good thermal stability, chemical stability, tunability, and good mechanical properties. Under nonhumidifying conditions, PIL-based membranes show a conductivity up to the order of 1×10^{-1} S/cm at 160 °C, due to the well-connected PIL nanochannels preserved in the membrane. This type of polymer conducting membranes have potential application in high-temperature polymer electrolyte membrane fuel cells.

Introduction

Polymer electrolyte membrane fuel cells (PEMFCs) are a type of fuel cells which use a proton conducting polymer membrane as the electrolyte. They are attracting a great deal of interest because of their high power density, high energy-conversion efficiencies, low starting temperature, and easy handling.¹ More recently, operation of PEMFCs at elevated temperature (>100 °C) has been receiving increased attention because it will enhance reaction kinetics at both electrodes, improve the carbon monoxide tolerance of the platinum catalyst at the anode, and simplify heat and humidity managements of PEMFCs.² However, at present, the most commonly used humidified perfluorinated ionomer membranes, represented by Nafion, are limited to being used at temperatures lower than 100 °C because of the evaporation of water, which results in a rapid loss of conductivity. Several approaches, such as incorporation of hydrophilic inorganic fillers into the polymer electrolyte membranes,³ use of chemical cross-linking agents,⁴ and development of new types of membranes⁵ different than Nafion membranes, have

been pursued to obtain polymer electrolyte membranes with high thermal stability and good water retention. However, few substances can retain water above 130 °C. As an alternative method, replacement of water with nonaqueous, low-volatility proton carriers, such as phosphoric acid⁶ and protic ionic liquids (PILs),⁷ is particularly advantageous for fuel cells at elevated temperatures under anhydrous conditions.

Protic ionic liquids, which could be easily produced through the combination of a Brønsted acid and Brønsted base, have attracted considerable attention because of their unique properties such as negligible volatility and high

* Corresponding author. E-mail: fyan@suda.edu.cn; lujm@suda.edu.cn.

† Soochow University.

‡ Fudan University.

§ Chinese Academy of Sciences.

- (1) (a) Perry, M. L.; Fuller, T. F. *J. Electrochem. Soc.* **2002**, *149*, S59–67. (b) Dresselhaus, M. S.; Thomas, I. L. *Nature (London)* **2001**, *414*, 332–337. (c) Yang, Z.; Rajendran, R. G. *Angew. Chem., Int. Ed.* **2005**, *44*, 564–567. (d) Kreuer, K.-D.; Paddison, S. J.; Spohr, E.; Schuster, M. *Chem. Rev.* **2004**, *104*, 4637–4678.
- (2) (a) Rikukawa, M.; Sanui, K. *Prog. Polym. Sci.* **2000**, *25*, 1463–1502. (b) Kreuer, K. D. *ChemPhysChem* **2002**, *3*, 771–775. (c) Alberti, G.; Casciola, M. *Solid State Ionics* **2001**, *145*, 3–16. (d) Yamada, M.; Honma, I. *J. Phys. Chem. B* **2004**, *108*, 5522–5526. (e) Adjemian, K. T.; Lee, S. J.; Srinivasan, S.; Benziger, J.; Bocarsly, A. B. *J. Electrochem. Soc.* **2002**, *149*, A256–A261.

- (3) (a) Nunes, S. P.; Ruffmann, B.; Rikowski, E.; Vetter, S.; Richau, K. *J. Membr. Sci.* **2002**, *203*, 215–225. (b) Yang, C.; Constamagna, P.; Srinivasan, S.; Benziger, J.; Bocarsly, A. B. *J. Power Sources* **2001**, *103*, 1–9. (c) Damay, F.; Klein, L. C. *Solid State Ionics* **2003**, *162*, 261–267. (d) Su, Y.-H.; Liu, Y.-L.; Sun, Y.-M.; Lai, J.-Y.; Guiver, M. D.; Gao, Y. *J. Power Sources* **2006**, *155*, 111–117. (e) Mecheri, B.; Epifanio, A. D.; Vona, M. L. D.; Traversa, E.; Licoccia, S.; Miyayama, M. *J. Electrochem. Soc.* **2006**, *153*, A463–A467.
- (4) (a) Kerres, J. A. *Fuel Cells* **2005**, *5*, 230–247. (b) Lee, C. H.; Park, H. B.; Chung, Y. S.; Lee, Y. M.; Freeman, B. D. *Macromolecules* **2006**, *39*, 755–764. (c) Xing, P.; Robertson, G. P.; Guiver, M. D.; Mikhailenko, S. D.; Wang, K.; Kaliaguine, S. *J. Membr. Sci.* **2004**, *229*, 95–106. (d) Mikhailenko, S. D.; Wang, K.; Kaliaguine, S.; Xing, P.; Robertson, G. P.; Guiver, M. D. *J. Membr. Sci.* **2004**, *233*, 93–99.
- (5) (a) Khiterer, M.; Loy, D. A.; Cornelius, C. J.; Fujimoto, C. H.; Small, J. H.; McIntire, T. M.; Shea, K. J. *Chem. Mater.* **2006**, *18*, 3665–3673. (b) Tezuka, T.; Tadanaga, K.; Hayashi, A.; Tatsumisago, M. *J. Am. Chem. Soc.* **2006**, *128*, 16470–16471. (c) Miyatake, K.; Zhou, H.; Watanabe, M. *Macromolecules* **2004**, *37*, 4956–4960. (d) Vona, Di M. L.; Sgreccia, E.; Licoccia, S.; Khadhraoui, M.; Denoyel, R.; Knauth, P. *Chem. Mater.* **2008**, *20*, 4327–4334. (e) Hickner, M. A.; Ghassemi, H.; Kim, Y. S.; Einsla, B. R.; McGrath, J. E. *Chem. Rev.* **2004**, *104*, 4587–4612.
- (6) (a) Kreuer, K. D. *Chem. Mater.* **1996**, *8*, 610–641. (b) Li, Q.; He, R.; Jensen, J. O.; Bjerrum, N. J. *Fuel Cells* **2004**, *4*, 147–159. (c) Weber, J.; Kreuer, K. D.; Maier, J.; Thomas, A. *Adv. Mater.* **2008**, *20*, 2595–2598. (d) Mecerreyes, D.; Grande, H.; Miguel, O.; Ochoteco, E.; Marcilla, R.; Cantero, I. *Chem. Mater.* **2004**, *16*, 604–607.

thermal stability. One of the characteristic features of PILs is their ability to form hydrogen bonds, and the proton conductivity of PILs has been experimentally proven in the H₂/O₂ cells under nonhumidifying conditions.^{7d–g} Compared with water, a benefit of using PILs as proton electrolytes for PEMFCs is that the cells can be operated at temperatures higher than 100 °C under anhydrous conditions. From a practical perspective, solid or semisolid conductive electrolytes with good mechanical strength are generally preferred over fluidic materials. Thus, it is desirable to convert PIL-based electrolyte solutions into a solid or quasi-solid form. Scrosati,^{8a} Fornicola,^{8b} and Martinelli^{8c} recently synthesized proton-conducting membranes by incorporating a PIL into a poly(vinylidenefluoride-co-hexafluoropropylene) (PVdF) polymer matrix.⁸ The obtained polymer electrolyte membranes show high thermal stability, high ionic conductivity, and are proposed as new polymer electrolyte membranes for high-temperature PEMFCs. Because fluorinated polymers are generally expensive and have a great danger to the environment, preparation of alternative polymer electrolyte membranes with relatively cheap, nonfluorinated polymeric materials is in great demand.⁹

The successful preparation of IL-based polymer electrolytes, however, is critically dependent on the compatibility of ILs and polymeric matrix. Only a few IL-based polymer gels, other than PVdF polymer matrix, have been recently reported.^{10c} Because the factors responsible for the miscibility of IL-based polymer systems are complex, it is still difficult to predict the compatibility of ILs with a polymeric matrix.^{10,11} This obstacle may be overcome in some cases through the polymerization of IL-based microemulsions.¹¹

Microemulsions are thermodynamically stable dispersions containing two immiscible liquids stabilized by surfactants at the liquid–liquid interface. Polymerization of a bicontinuous microemulsion produces bicontinuous nanostructures

throughout the polymeric material, which may be suitable for polymer electrolyte membranes.¹² IL-based microemulsions, in which an IL dispersed in an oil-continuous phase stabilized by suitable surfactants, behavior consistent with water-in-oil microemulsions and provide nanosized IL domains as reaction or extraction media.¹³ This type of microemulsions are attracting great interest because of the unique features of both IL and microemulsion system. However, polymerization of IL-based microemulsions, especially of PIL-based microemulsions, has not yet been intensively studied.^{11a}

We were motivated in this study to prepare the proton conducting membranes via the polymerization of microemulsions containing nanostructured PIL networks. It is expected that PIL nanostructures formed in the precursor microemulsions could be preserved in the resultant polymeric matrix without macroscopic phase separation, even if the produced vinyl polymers are incompatible with PIL cores. The preserved PIL networks in the composite membranes, therefore, will enhance the proton conductivity of membranes. The concept provided in this work combines the advantages of both the polymerization of microemulsions and the properties of PILs.

Experimental sections

Materials. Styrene, acrylonitrile, *N*-ethylimidazole, 1,2-dimethylimidazole, *N*-methylimidazole, trifluoromethanesulfonic acid, divinylbenzene, benzoinisobutyl ether, tetrahydrofuran, acetonitrile, diethyl ether, and ethyl acetate were used as purchased. All of the vinyl monomers were made inhibitor-free by passing the liquid through a column filled with Al₂O₃. Distilled deionized water was used for all experiments.

Synthesis. Protic ionic liquids were synthesized by mixing of an imidazole derivative with equivalent molar amount of trifluoromethanesulfonic acid, as documented in the literature.^{8a} The details of synthesis and characterization of PILs were depicted in the Supporting Information. Polymerizable surfactant, 1-(2-methyl acryloyloxyundecyl)-3-methyl imidazolium bromide (MAUM-Br) was synthesized according to the procedures reported previously.¹¹

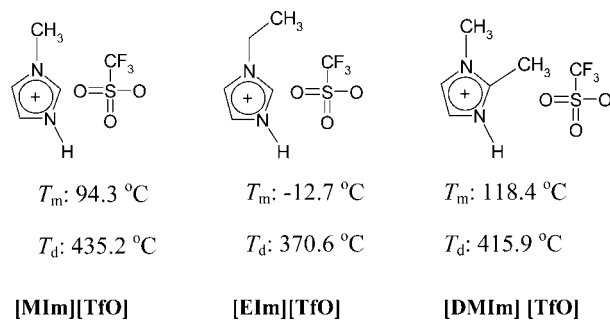
Polymerization of Microemulsion. The single-phase domains of PIL/surfactant/monomer microemulsions were determined visually on the basis of transparency and absence of phase separation in PTFE-lined, screw-capped culture tubes. Polymerization of PIL-based microemulsions was conducted in a glass mold by irradiation with UV-light of 250-nm wavelength.

Characterization. Thermal analysis was carried out by Universal Analysis 2000 thermogravimetric analyzer (TGA). A temperature ramp of 10 °C/min was applied under nitrogen flow. Dynamic mechanical analysis (DMA) measurements of PIL-based composite membranes were conducted with a TA DMA Q 800. The samples were heated from 30 to 180 °C at a heating rate of 5 °C/min. The sample chamber was purged with nitrogen at 20 mL/min throughout the test. Phase-lag atomic force microscopy (AFM) images were measured with a NT-MDT Solver P47 AFM in a semicontact mode. The oscillation frequency was set to approximately 255 kHz with Si cantilever which had a spring constant of about 11.5 N/m. Small

- (7) (a) Belieres, J.-P.; Gervasio, D.; Angell, C. A. *Chem. Commun.* **2006**, 4799–4801. (b) Greaves, T. L.; Drummond, C. J. *Chem. Rev.* **2008**, 108, 206–237. (c) Martinelli, A.; Matic, A.; Jacobsson, P.; Börjesson, L.; Navarra, M. A.; Panero, S.; Scrosati, B. *J. Electrochem. Soc.* **2007**, 154, G183–187. (d) Susan, Md. A. B. H.; Noda, A.; Mitsushima, S.; Watanabe, M. *Chem. Commun.* **2003**, 938–939. (e) Noda, A.; Susan, Md. A. B. H.; Kudo, K.; Mitsushima, S.; Hayamizu, K.; Watanabe, M. *J. Phys. Chem. B* **2003**, 107, 4024–4033. (f) Nakamoto, H.; Noda, A.; Hayamizu, K.; Hayashi, S.; Hamaguchi, H.; Watanabe, M. *J. Phys. Chem. C* **2007**, 111, 1541–1548. (g) Fornicola, A.; Scrosati, B.; Ohno, H. *Ionics* **2006**, 12, 95–102. (h) Gu, H.; England, D.; Yan, F.; Texter, J. *2nd IEEE International Nanoelectronics Conference*; Shanghai, March 24–27, 2008; IEEE: Piscataway, NJ, 2008; pp 863–868.
- (8) (a) Fornicola, A.; Panero, S.; Scrosati, B.; Tamada, M.; Ohno, H. *ChemPhysChem* **2007**, 8, 1103–1107. (b) Fornicola, A.; Panero, S.; Scrosati, B. *J. Power Sources* **2008**, 178, 591–595. (c) Martinelli, A.; Matic, A.; Jacobsson, P.; Börjesson, L.; Fornicola, A.; Panero, S.; Scrosati, B.; Ohno, H. *J. Phys. Chem. B* **2007**, 111, 12462–12467. (d) Navarra, M. A.; Panero, S.; Scrosati, B. *Electrochem. Solid-State Lett.* **2005**, 8, A324.
- (9) (a) Miyatake, K.; Tombe, T.; Chikashige, Y.; Uchida, H.; Watanabe, M. *Angew. Chem., Int. Ed.* **2007**, 46, 6646–6649. (b) Ye, H.; Huang, J.; Xua, J. J.; Kodiweera, N. K. A. C.; Jayakody, J. R. P.; Greenbaum, S. G. *J. Power Sources* **2008**, 178, 651–660.
- (10) (a) Snedden, P.; Cooper, A. I.; Scott, K.; Winterton, N. *Macromolecules* **2003**, 36, 4549–4556. (b) Susan, M. A.; Kaneko, T.; Noda, A.; Watanabe, M. *J. Am. Chem. Soc.* **2005**, 127, 4976–4983, and references therein. (c) Yan, F.; Texter, J. *Prog. Polym. Sci.* **2009**, doi:10.1016/j.progpolymsci.2008.12.001.
- (11) (a) Yu, S.; Yan, F.; Zhang, X.; You, J.; Wu, P.; Lu, J.; Xu, Q.; Xia, X.; Ma, G. *Macromolecules* **2008**, 41, 3389–3392. (b) Yan, F.; Texter, J. *Chem. Comm.* **2006**, 2696–2699. (c) Yan, F.; Texter, J. *Angew. Chem., Int. Ed.* **2007**, 46, 2440–2443.

- (12) Yan, F.; Texter, J. *Soft Matter* **2006**, 2, 109–118.
- (13) (a) Eastoe, S.; Gold, S. E.; Rogers, A.; Paul, T.; Welton, R. K.; Heenan, I. G. *J. Am. Chem. Soc.* **2005**, 127, 7302–7303. (b) Gao, H. X.; Li, J. C.; Han, B. X.; Chen, W. N.; Zhang, J. L.; Zhang, R.; Yan, D. *Phys. Chem. Chem. Phys.* **2004**, 6, 2914–2916.

Scheme 1. Molecular Structures and Thermal Properties (melting temperature T_m and decomposition temperature T_d) of PILs Developed in This Work



pieces were cut from each membrane, which have a thickness of about 500 μm , and glued onto sample disks. All the AFM images were undertaken at room temperature.

The resistance of the PIL-based polymer membranes was measured by the AC impedance method over the frequency range 1 Hz to 1 MHz using electrochemical workstations (Zahner IM6EX). A rectangular piece of membrane was sandwiched between two gold electrodes in a glass cell and placed in a programmable oven to measure the temperature dependence of the conductivity. The membranes were dried at 100 $^\circ\text{C}$ for 8 h under a vacuum and taken out just before conductivity measurement in an effort to keep the samples dry. Before the measurements at each temperature set point, the samples were held at constant temperature for at least 10 min.

Results and Discussion

PILs were synthesized by neutralizing imidazole derivatives with trifluoromethanesulfonic acid. Scheme 1 shows the molecular structure and thermal properties of N-methylimidazolium trifluoromethanesulfonate ([MIm][TfO]), N-ethylimidazolium trifluoromethanesulfonate ([EIm][TfO]) and 1,2-dimethylimidazole trifluoromethanesulfonate ([DMIIm][TfO]) developed in this work. The purity and chemical structure of the PILs were confirmed by ^1H NMR measurements as described in the Supporting Information.

Styrene, which is widely available monomer was first chosen as a polymerizable oil to form PIL-based microemulsions. However, polystyrenes are susceptible to be attacked by hydroperoxide radical species during the fuel cell applications because of the weakness of the benzylic α -hydrogen atom.¹⁴ The chemical stability of polystyrenes could be improved by grafting or copolymerization of styrene with acrylonitrile;^{14b,c} therefore, a mixture of styrene and acrylonitrile was used as an oil phase to prepare PIL-based microemulsions in this work. A polymerizable surfactant, 1-(2-methyl acryloyloxyundecyl)-3-methyl imidazolium bromide (MAUM-Br) was synthesized and used as a stabilizer for PIL/monomer microemulsions.¹¹ The partial phase diagrams of PIL/MAUM-Br/styrene/acrylonitrile ternary system at 24 $^\circ\text{C}$ are illustrated in the Supporting Information. Microemulsions consisting of PIL (45 wt %), styrene (18.5 wt %), acrylonitrile (10.5 wt %), MAUM-Br (26 wt %),

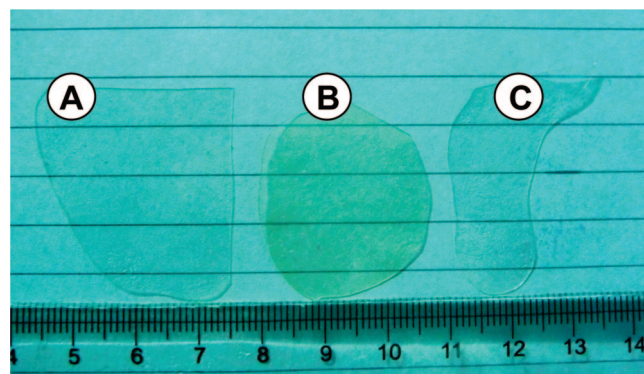


Figure 1. Photographs of PIL-based polymer composite membranes containing 45 wt % (A) [MIm][TfO], (B) [EIm][TfO], and (C) [DMIIm][TfO]. Membrane thickness $\approx 60\text{ }\mu\text{m}$.

divinylbenzene (4 wt % to the formulation, based on the weight of monomer and polymerizable surfactant) and 0.5 wt % of photoinitiator benzoinisobutyl ether were cross-linked by irradiation with UV light of 250 nm wavelength in a mold.

Figure 1 shows the photographs of produced PIL-based polymeric composite membranes. Even though the resulting vinyl copolymers are incompatible with PIL phases, the obtained composite membranes are free-standing, transparent, and no apparent visible phase separation was observed during and after the polymerization process. These membranes are flexible and can be cut into any desired sizes and shapes, whereas the pure form polymeric matrix (without PILs) is stiff and brittle. Dynamic mechanical analysis (DMA) of the membranes containing 45 wt % [MIm][TfO], [EIm][TfO], and [DMIIm][TfO] shows the storage modulus of 3.7, 8.6, and 8.4 MPa at 30 $^\circ\text{C}$, which decrease to 0.91, 0.73, and 0.67 MPa at 160 $^\circ\text{C}$, respectively. It is not surprising that the storage modulus of the membrane can be increased to ~ 10 times higher when the cross-linker content was increased from 4 to 8 wt %. Thermogravimetric analyzer (TGA) data (see the Supporting Information) reveal that all the membranes lose less than 10% in weight up to 300 $^\circ\text{C}$, confirming that this type of PIL-based membranes indeed confer a high thermal stability, far beyond the range of interest for application in PEMFCs.

Figure 2 shows the phase-lag atomic force microscopy (AFM) images of the fracture cross section of polymer composite membranes, revealing the morphology and the PIL distribution in the membranes. Changes in the phase lag reflect changes of composition, hardness, friction, viscoelasticity and etc. Minimal correlation of height images (Figure 2B, D, F) indicate that phase-lag images (Figure 2A, C, E) are unlikely to be an artifact of surface roughness. Images A, C, and E in Figure 2 clearly show the bicontinuous and randomly distributed PIL nanochannels and polymer nanodomains. The domain widths of each channel were in the range of 20–50 nm (tubule diameter). The morphological features qualitatively explain why the PIL-based composite membranes are transparent and flexible even though polymeric matrix and PILs are incompatible with each other.

Ionic conductivity of PIL-based polymer composite membranes was measured with an alternating current impedance spectroscopy in a closed cell under anhydrous conditions.

(14) (a) Becker, W.; Schmidt-Naake, G. *Chem. Eng. Technol.* **2001**, *24*, 1128–1132. (b) Becker, W.; Bothe, M.; Schmidt-Naake, G. *Die Angew. Makromol. Chem.* **1999**, *273*, 57–62. (c) Gubler, L.; Gursel, S. A.; Scherer, G. G. *Fuel Cells* **2005**, *5*, 317–335.

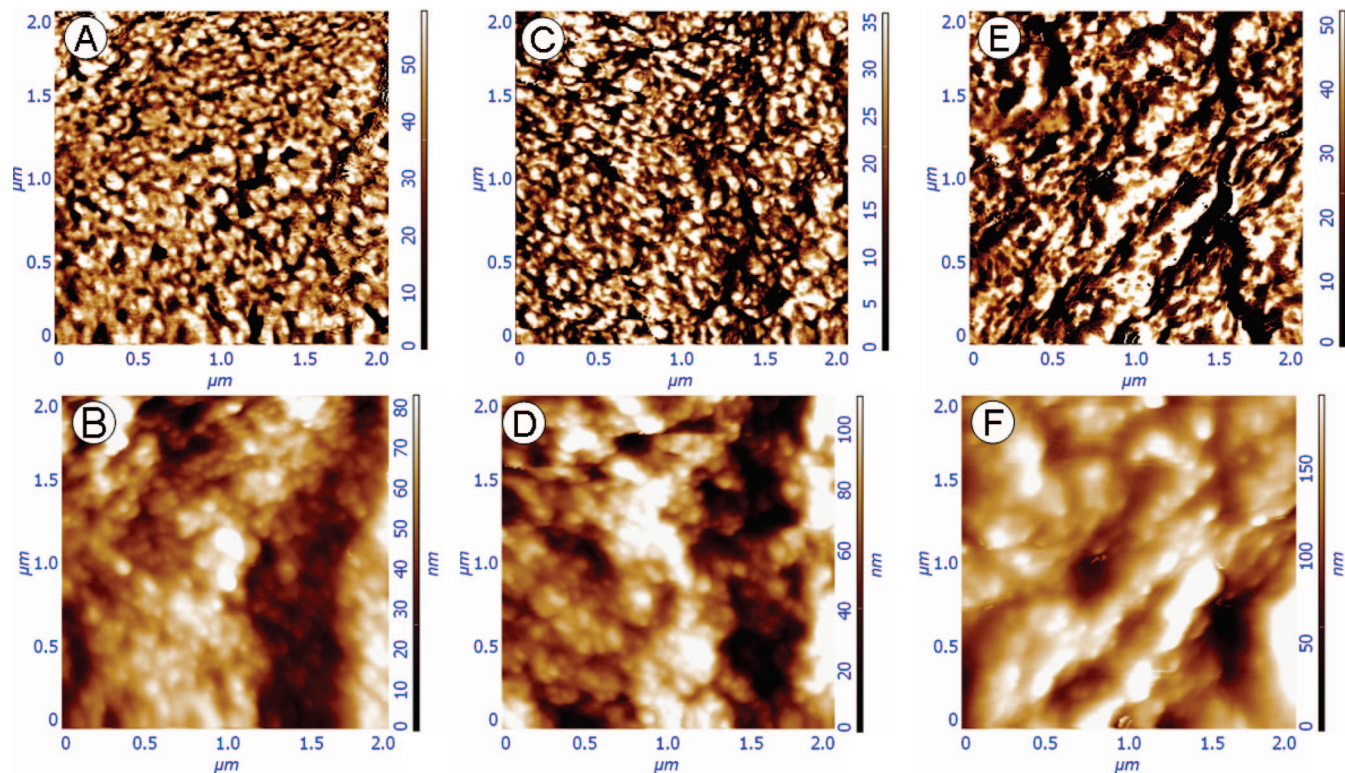


Figure 2. AFM phase (A, C, E) and height (B, D, F) images of the fracture cross-section of the PIL-based polymer composite membranes containing 45 wt % (A, B) [MIm][TfO], (C, D) [EIm][TfO], and (E, F) [DMIm][TfO], respectively. Each image frame is $2 \mu\text{m} \times 2 \mu\text{m}$.

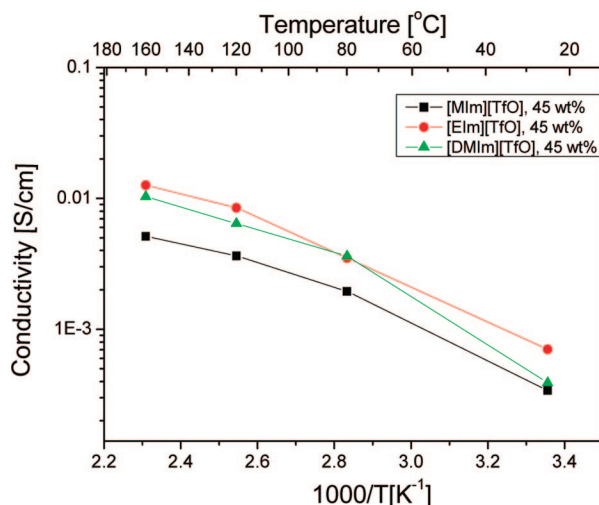


Figure 3. Conductivity Arrhenius plots of the PIL-based polymer composite membranes containing 45 wt % PILs.

Figure 3 shows the reproducible plot of ionic conductivity of polymer membranes containing 45 wt % [MIm][TfO], [EIm][TfO], and [DMIm][TfO], exhibiting conductivity of 3.48×10^{-4} S/cm at 20°C , respectively. The composite membranes shows similar temperature dependent conductivity and following Vogel–Tamman–Fulcher (VTF) behavior, which indicate that these membranes have similar proton conduction mechanism, that is, a proton vehicle movement associated with the translation of the protonated imidazole units.^{6c,7b,8a,15} All the samples show no decay in conductivity even at the temperature as high as 160°C , reaching values of 5.51×10^{-3} , 1.27×10^{-2} , and 1.03×10^{-2} S/cm, respectively (Figure 3).

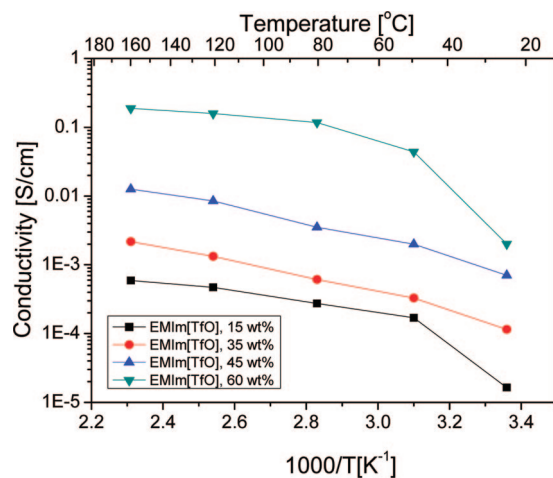


Figure 4. Conductivity Arrhenius plots of the [EIm][TfO]/polymer membranes.

The conductivity also increases when the PIL content is increased (Figure 4). The membrane containing 60 wt % [EIm][TfO] shows a conductivity of 1.93×10^{-1} S/cm at 160°C , which is about 300 times higher than that of the membrane containing 15 wt % [EIm][TfO] (5.8×10^{-4} S/cm) under the same experimental conditions. Watanabe,^{9a} Thomas,^{6c} and Mecerreyres^{6d} recently demonstrated that introduction of a well-defined biphasic nanostructure into the polymer electrolyte membrane could significantly improve proton conductivity. Therefore, the huge difference in the conductivity for two membranes can be explained by missing biphasic nanostructures in the case of the membrane with lower loading, in which PILs are discretely dispersed in the polymeric matrix.¹¹ On the other hand, PILs are well-

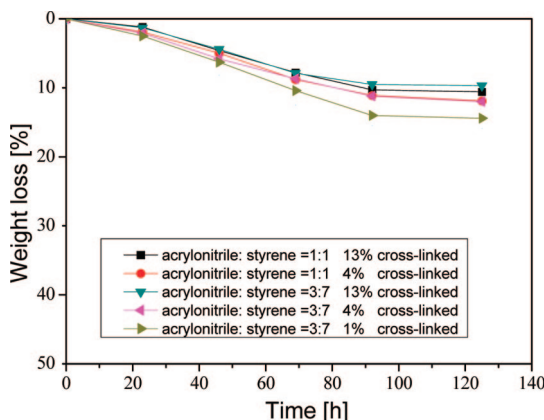


Figure 5. Polymer membranes degradation in 3% H_2O_2 containing 4 ppm Fe^{2+} at 68 $^{\circ}\text{C}$.

interconnected within the nanochannels in membranes and act as a proton transporting pathway in the composite membrane with higher loading. The results observed here clearly demonstrate the benefit of interconnected PIL nanostructures formed in the membranes.^{15b}

Chemical stability of polymer electrolyte membranes is of much concern to the lifetime of PEMFCs. The stability of the polymer electrolyte membranes in Fenton's reagent (solution containing H_2O_2 and transition metal ions) has been recognized as an important indication of the durability of the membranes in fuel cells.^{1d,16} Figure 5 shows the degradation of pure form (without PILs) of polymer membranes tested in Fenton's reagent (3% H_2O_2 solution containing 4 ppm Fe^{2+}) at 68 $^{\circ}\text{C}$. The degradation of polymer membranes is evaluated by the weight loss and visual observation. In the first 20 h, about 2% weight loss was observed for the polymer membranes prepared on the basis of the formulation shown in Figure 5. However, none of the membranes was broken into small pieces, and all of the samples remained in a good membrane form even after a 130 h testing period (9–15% weight loss). Chemical stability of polymers can be improved with increase in the cross-linker content. As can be seen in Figure 5, the weight loss was 15, 12, and 9% for polymer membranes (3:7 acrylonitrile:styrene molar ratio in the microemulsion formulation) with cross-linking degrees of 1, 4, and 13%, respectively. It should be noted that the chemical stability of the polymer membrane prepared from a microemulsion containing 13 wt % cross-linker is even comparative to that of Nafion 117 membranes (which showed

(15) (a) Susan, M. A. B. H.; Noda, A.; Mitsushima, S.; Watanabe, M. *Chem. Commun.* **2003**, 938–939. (b) Ye, H.; Huang, J.; Xu, J. J.; Kadiweera, N. K. A. C.; Jayakody, J. R. P.; Greenbaum, S. G. *J. Power Sources* **2008**, *178*, 651–660.
 (16) Li, Q.; Pan, C.; Jensen, J. O.; Noyé, P.; Bjerrum, N. J. *Chem. Mater.* **2007**, *19*, 350–352.

weight loss of ~9%) after a 100 h test under the same experimental conditions.¹⁶ An increase in acrylonitrile content in the microemulsion formulation does not improve chemical stability of the prepared polymer membranes.

Conclusion

In summary, we report here the first example of an effective approach to prepare the nonaqueous proton conducting membranes via the polymerization of microemulsions comprising surfactant-stabilized PIL nanodomains. The resultant polymer electrolyte membranes are uniform, transparent and flexible even though the resulting vinyl polymers are immiscible with PIL cores. These PIL-based polymer membranes have quite a good thermal stability, chemical stability, tunability, and good mechanical properties. Under nonhumidifying conditions, the produced polymer electrolyte membranes have conductivity up to the order of 1×10^{-1} S/cm at 160 $^{\circ}\text{C}$ because of the well-connected PIL nanochannels formed in the samples. The above-described results demonstrate that the PIL-based membranes present in this work combine the high proton conductivity and good mechanical properties in a unique way. We believe this type of composite membranes should have an impact on further investigations in the field of proton conducting membranes for PEMFCs, and the methodology presented in this work could be extendable to other liquid monomers and PILs with desirable properties for the preparation of nonfluorinated polymer electrolyte membranes.

However, the long-term operation of the PIL-based membranes could be affected by a progressive release of the PIL. Further improvements to retain the PIL component upon cell operation must be carefully considered. We assume that the design and synthesis of polymer matrices that could anchor the PIL component into the membrane should be one of the most effective ways. Consequently, the elucidation of interaction between the polymeric matrix and PILs need to be further explored in future work.

Acknowledgment. This work was supported by Natural Science Foundation of China (20774063, 20874071, 20876101), the Program for New Century Excellent Talents in University (Grant NCET-07-0593), and Fok Ying Tung Education Foundation (114022).

Supporting Information Available: Synthesis and characterization of protic ionic liquids, partial phase diagrams of the microemulsions, and TGA data of polymer membranes (PDF). This material is available free of charge via the Internet at <http://pubs.acs.org>.

CM900098R